Rapid Communications

Rotating mixed ^{3}He - ^{4}He nanodroplets

Martí Pi,[1,2] Francesco Ancilotto,[3,4] José María Escartín,[5] Ricardo Mayol,[1] and Manuel Barranco[1,2,6]

[1]*Departament FQA, Facultat de Física, Universitat de Barcelona, Diagonal 645, 08028 Barcelona, Spain*

[2]*Institute of Nanoscience and Nanotechnology (IN2UB), Universitat de Barcelona, 08028 Barcelona, Spain*

[3]*Dipartimento di Fisica e Astronomia "Galileo Galilei" and CNISM, Università di Padova, via Marzolo 8, 35122 Padova, Italy*

[4]*CNR-IOM Democritos, via Bonomea, 265-34136 Trieste, Italy*

[5]*Institut de Química Teòrica i Computacional, Universitat de Barcelona, Carrer de Martí i Franquès 1, 08028 Barcelona, Spain*

[6]*Université Toulouse 3, Laboratoire des Collisions, Agrégats et Réactivité, IRSAMC, 118 Route de Narbonne, F-31062 Toulouse Cedex 09, France*

(Received 17 March 2020; revised 23 July 2020; accepted 24 July 2020; published 7 August 2020)

Mixed ^{3}He - ^{4}He droplets may acquire angular momentum during their passage through the nozzle of the experimental apparatus, cooling down and undergoing isotopic segregation, developing a ^{3}He crust surrounding a superfluid ^{4}He core. Within density functional theory, we investigate their stability and the relations between their angular momenta and their shapes. We uncover a variety of behaviors where the interplay between the superfluid ^{4}He core and the normal-fluid ^{3}He coating leads to a scenario that both bears analogies with viscous rotating drops and displays new features such as configurations with a fissioned or three-lobed ^{4}He core, or with multiply charged vortices.

DOI: 10.1103/PhysRevB.102.060502

Ordinary liquids are known to form drops held together by surface tension. When they are set into rotation, their spherical shape experiences large deformations, evolving from oblate to prolate and two-lobed, eventually fissioning if the rotational velocity is large enough [1]. The appearance and stability of, e.g., rotating celestial bodies [2], atomic nuclei [3], and tektites [4], to cite some quite different objects, has been found to bear similarities with rotating classical drops, adding an extrinsic interest to their study.

Helium, in its two isotopes ^{4}He and ^{3}He, is the only element in nature that may remain liquid and form droplets at temperatures (T) close to absolute zero [5]. Both isotopes may be superfluid, with normal-to-superfluid transition temperatures of 2.17 K (^{4}He) and 2.7 mK (^{3}He). At the temperatures of helium droplet experiments, 0.37 K for ^{4}He [6] and 0.15 K for ^{3}He [7], ^{3}He is a normal fluid whereas ^{4}He is superfluid. They constitute an ideal testground to study how superfluidity affects rotation, as they are isolated quantum systems formed by atoms subject to the same bare interaction.

Rotating superfluid ^{4}He droplets made of $N_4 = 10^8$–10^{10} atoms, produced by hydrodynamic instability of a cryogenic fluid jet, have been studied by coherent x-ray scattering [8], revealing the presence of vortex lattices through the observation of Bragg patterns produced by Xe clusters captured by the vortex lines. Coherent diffractive imaging experiments using extreme ultraviolet pulses have also been carried out, aimed at providing information about the droplet shapes [9,10]. Surprisingly, these studies have shown that superfluid ^{4}He droplets follow the same shape sequence as rotating droplets made of viscous fluid do. It has been shown that this is due to the presence of quantized vortices and capillary waves, whose interplay confers on the superfluid droplet the appearance of a classical rotating object [11–13]. Until now, a deeper knowledge of how superfluid droplets rotate has been hampered by the experimental difficulty of determining their angular momentum, which is usually unknown [12]. This prevents a detailed comparison with theoretical models and the disclosure of the precise quantum nature of such rotation. Similar studies have been conducted very recently for rotating pure ^{3}He droplets [14]. These droplets are nonsuperfluid and behave very much as classical rotating droplets [15].

In liquid-helium mixtures characterized by the ^{3}He fraction $x_3 = N_3/N$, with $N = N_3 + N_4$, the normal-to-superfluid transition temperature decreases with increasing x_3 [16]. At low T, the mixture undergoes a two-phase separation where a pure ^{3}He phase coexists with a very ^{4}He-rich mixture [16]. These properties are transferred to the mixed droplets, which at the experimental T—sensibly that of pure ^{3}He droplets [17]—experience a two-phase separation yielding a core-shell structure, with a crust made of ^{3}He atoms in the normal state and a superfluid core mostly made of ^{4}He atoms [18]. This segregation has been instrumental in finding the minimum number of ^{4}He atoms needed to display superfluidity [17].

The ability to form self-bound isolated droplets made of a superfluid core enveloped by a normal-fluid shell is a unique characteristic of liquid-helium mixtures at very low temperatures. Bose-Einstein condensates (BECs) immersed in a Fermi sea have been observed [19], but these systems are not self-bound, and only exist confined by an external trap to which the droplets adapt their shape; self-bound droplets made of mixtures of bosonic cold gases have been also observed [20,21], and self-bound Bose-Fermi droplets have been studied theoretically [22]. However, cold-gas mixtures do not exist as phase-separated Bose-Fermi droplets, as they must remain in a mixed configuration to be self-bound [23].

The mixed normal-fluid–superfluid structure of ^{3}He - ^{4}He droplets is expected to affect their structural properties when they are set into rotation. A recent study addresses theoretically the classical rotation of droplets made of two immiscible viscous fluids [24]; when one component is superfluid, a quantum description is in order. We provide here such a description.

We have considered mixed helium droplets at "zero temperature," i.e., a temperature so low (a few millikelvin) that thermal effects on the energetics and morphology of the droplet are negligible, ^{3}He is in the normal phase, and ^{4}He is superfluid. We have taken as a case of study a $^4\mathrm{He}_{1500} + {}^3\mathrm{He}_{6000}$ nanodroplet ($x_3 = 80\%$). It has been chosen (within the limitations imposed by the unavoidable computational cost of the calculations) for physical reasons: a thick ^{3}He crust is needed to model a deformable container inside which the superfluid ^{4}He core may undergo different shape transitions; a thin crust would just adapt to the deforming core and one should not expect a phenomenology much different from that of pure ^{4}He droplets [11]. At the same time, the superfluid ^{4}He inner droplet must be large enough to host a number of quantized vortices [11]. In superfluid helium mixtures the vortex cores are filled with ^{3}He and, depending on x_3, their radius can be up to five times larger than for pure ^{4}He [25,26]. For the chosen N_4 value, the number of vortices (n_v) is expected to be small.

The droplets are described within the density functional theory (DFT) approach [27,28]. The fermionic shell structure of the droplet crust is smeared out due to the large number of ^{3}He atoms, and for this reason ^{3}He can be treated semiclassically in the Thomas-Fermi approximation [15]. The DFT equations obtained by functional variation of the energy density are formulated in a rotating frame of reference with constant angular velocity ω around the z axis [11]. In terms of the DFT Hamiltonians $\mathcal{H}_3[\rho_3, \rho_4]$ and $\mathcal{H}_4[\rho_3, \rho_4]$ [27], they are

$$\left\{\mathcal{H}_3[\rho_3, \rho_4] - \frac{m_3}{2}\,\omega^2(x^2 + y^2)\right\}\Psi_3(\mathbf{r}) = \mu_3\Psi_3(\mathbf{r}),$$
$$\{\mathcal{H}_4[\rho_3, \rho_4] - \omega\hat{L}_4\}\Psi_4(\mathbf{r}) = \mu_4\Psi_4(\mathbf{r}), \tag{1}$$

where μ_3 (μ_4) is the ^{3}He (^{4}He) chemical potential, $\hat{L}_4$ is the z component of the ^{4}He angular momentum operator, and $\Psi_3(\mathbf{r})$ and $\Psi_4(\mathbf{r})$ are the real ^{3}He and complex ^{4}He effective wave functions related to the atom densities as $\Psi_3^2(\mathbf{r}) = \rho_3(\mathbf{r})$ and $|\Psi_4(\mathbf{r})|^2 = \rho_4(\mathbf{r})$. These equations have been solved adapting the 4HE-DFT BCN-TLS computing package [29] to the case of helium mixtures, imposing a given value of the total angular momentum per atom, which requires finding iteratively the value of ω. Vortices are nucleated in the ^{4}He core using the imprinting procedure [11]. The calculations have been carried out as a function of the angular momentum per atom, $\mathcal{L} = (L_3 + L_4)/N = \mathcal{L}_3 + \mathcal{L}_4$ (expressed in $\hbar$ units), in unit $\Delta\mathcal{L}$ steps although finer meshes have sometimes been used [26]. For a given $\mathcal{L}$, the stable configuration is that with the lowest energy including the rotational energy (Routhian, $\mathcal{R}$) [1]. Configurations with higher $\mathcal{R}$ for the same $\mathcal{L}$ are metastable.

We characterize the appearance of the ^{4}He core and ^{3}He crust by the distance of their sharp surfaces (defined, for each isotope, by the locus at which the density equals that of the bulk liquid divided by 2 [11,15]) to the center of mass of the droplet, denoting the distances along the x, y, and z axes as a_x, b_y, and c_z, respectively; the Cartesian axes coincide with the principal rotation axes [10,11,15]. Dimensionless angular momentum Λ and angular velocity Ω variables have been introduced [24] (see the Supplemental Material [26] for their definitions). As in the case of isotopically pure droplets [1,4,12,30], they are useful to scale the results to droplets of different size for a given composition and have been thoroughly used in this work.

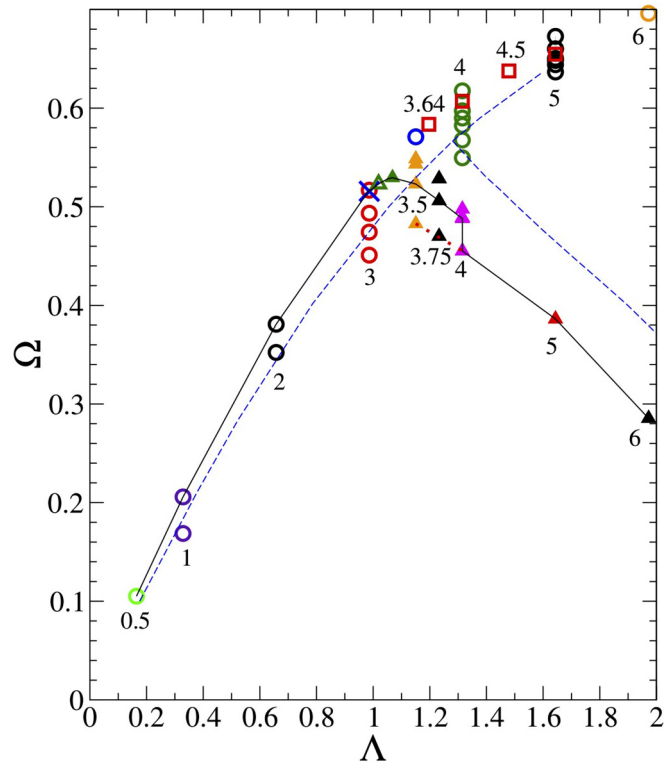

FIG. 1. Stability diagram in the Λ-Ω plane. Referring to the appearance of the outer surface of the ^{3}He shell: open circles, oblate configurations [Ω(Λ) rising branch]; triangles, prolate configurations [Ω(Λ) falling branch]; open squares, three-lobed ^{4}He core configurations. The cross indicates the oblate-to-prolate bifurcation point. The solid black line connects the stable configurations. The dotted red line shows the region of metastable fissioned ^{4}He core configurations. The dashed blue line is the DFT result for pure ^{3}He droplets [15]. The numbers close to the symbols indicate the value of the angular momentum per atom in units of $\hbar$. For further details see Table I of the Supplemental Material [26].

Figure 1 shows the stability diagram in the Λ-Ω plane. The solid line in Fig. 1 connects the stable, lowest-energy configurations. For a given Λ value, metastable configurations have been explored, which are also shown in Figs. 1–3 and discussed in the following. Figure 2 provides information on the shapes of the droplets through relationships between the geometrical parameters a_x, b_y, and c_z that characterize the shape of the outer ^{3}He surface [4,10], and Fig. 3 connects the shapes of the droplets with the dimensionless angular momentum Λ. The detailed

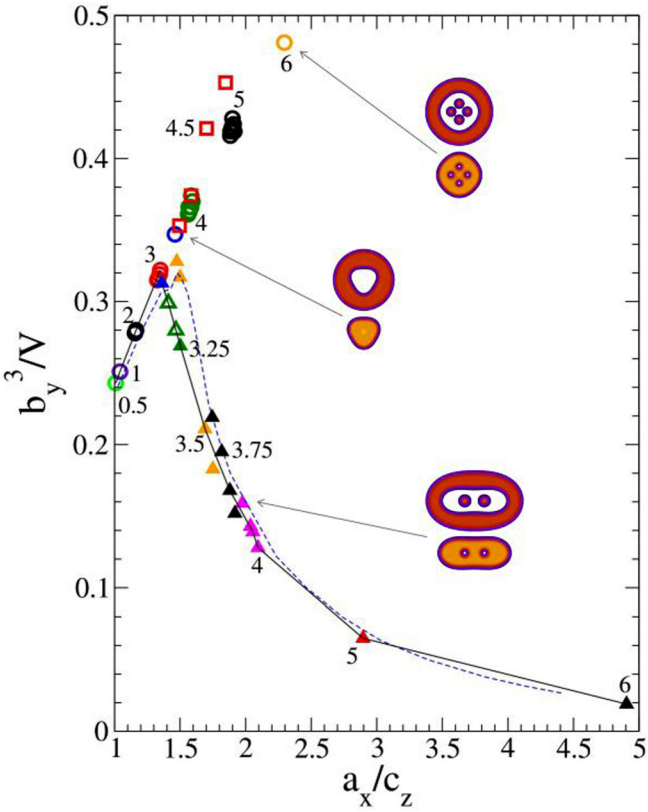

FIG. 2. Referring to the appearance of the outer surface of the ^{3}He shell, b_y^3/V ratio vs a_x/c_z, where V is the volume of the spherical droplet. Symbols and lines have the same meaning as in Fig. 1. The pictograms represent calculated ^{3}He (top) and ^{4}He (bottom) two-dimensional densities on the symmetry plane perpendicular to the rotational axis for selected configurations.

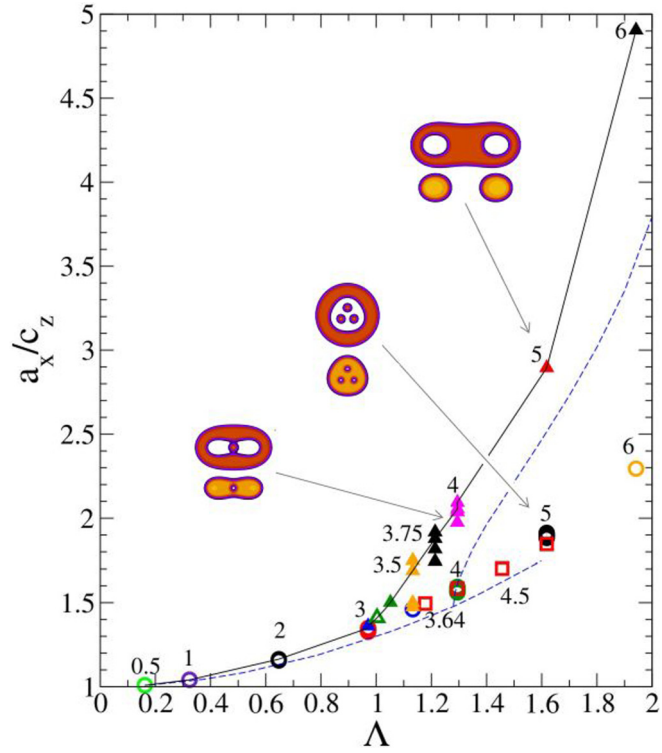

FIG. 3. a_x/c_z ratio of the outer surface of the ^{3}He shell vs Λ. Symbols, lines, and pictograms have the same meaning as in Fig. 2.

energetics and morphologic characteristics of the nanodroplet configurations are collected in Table I of the Supplemental Material [26].

Our study has unveiled a rich variety of stable and metastable configurations. As Λ increases from zero, the ^{3}He crust becomes oblate. At variance, the superfluid ^{4}He core remains spherical (see middle top panel in Fig. 4), becoming axisymmetric only when Λ is large enough. Since the superfluid ^{4}He core cannot be set into rotation around the symmetry axis because it is quantum-mechanically forbidden, at this stage the angular momentum of the droplet is efficiently stored in the ^{3}He shell, which acts as a rotating deformable container. We have found that this happens up to the oblate-to-prolate bifurcation point at $(\Lambda, \Omega) = (0.99, 0.52)$. Thus, oblate stable configurations are vortex-free for droplets of the size and composition studied here, although metastable vortex-hosting configurations do exist [26].

In the prolate branch, the outer surface of the ^{3}He crust is triaxial-ellipsoid-like up to $\Lambda \sim 1.64$, where it becomes two-lobed. At variance, the superfluid ^{4}He core becomes two-lobed at $\Lambda \sim 1.05$, i.e., immediately after bifurcation. This is due to the small surface tension of the ^{3}He - ^{4}He interface, 0.016 K Å^{-2}, as compared to that of the ^{3}He free surface, 0.113 K Å^{-2}. Pure ^{3}He droplets become two-lobed at $\Lambda = 1.85$ [15].

Prolate stable configurations with simply connected ^{4}He cores have been found only in a narrow angular momentum range $0.99 \leqslant \Lambda \leqslant 1.15$, where the core shape evolves from spheroidal to triaxial to two-lobed. Due again to the small surface tension of the ^{3}He - ^{4}He interface, the ^{4}He core undergoes fission when the ^{3}He crust is still triaxial-ellipsoid-like. The resulting stable prolate configuration consists of a fissioned ^{4}He core inside a rotating triaxial ^{3}He crust. The transition from simply connected to fissioned ^{4}He core configurations appears as a jump in the $\Omega(\Lambda)$ curve in Fig. 1 at $\Lambda = 1.31$; this could not be predicted out of simply connected shape models.

We have looked for prolate configurations with a fissioned ^{4}He core hosting a vortex in each moiety. After phase-imprinting them [11], vortices are eventually expelled in the course of the numerical relaxation; we conclude that these configurations are not stable for up to the largest Λ addressed in this study, $\Lambda = 1.97$.

The existence of *metastable* vortex-hosting configurations demonstrates that the droplet size we have chosen for this study would be large enough to accommodate vortices in the equilibrium configuration if this were energetically favorable, as is the case for pure ^{4}He droplets. We remark that the energy difference between metastable vortex-hosting and stable vortex-free configurations can be very small [26]. Both kinds of configurations are likely separated by small energy barriers, and one should not discard the idea that both could be detected in experiments.

Remarkably, we have found that along the metastable oblate branch, configurations with $n_v = 1$ have lower energy than vortex-free configurations. In this region, configurations hosting up to four vortices appear at $\Lambda > 1.15$. All these

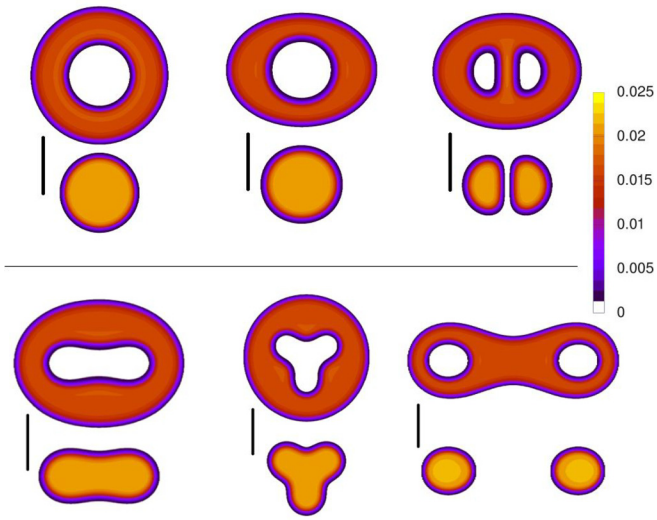

FIG. 4. Two-dimensional density of the $^4He_{1500}$ - $^3He_{6000}$ nanodroplet. Top: on a symmetry plane containing the rotational axis. From left to right, spherical configuration at $\Lambda = 0$; oblate vortex-free ^{4}He core configuration at $\Lambda = 0.99$, and oblate one-vortex configuration with quantum circulation $m = 1$ also at $\Lambda = 0.99$. Bottom: on the symmetry plane perpendicular to the rotational axis. From left to right, prolate vortex-free ^{4}He core configuration at $\Lambda = 1.15$, oblate three-lobed ^{4}He core configuration at $\Lambda = 1.32$, and prolate fissioned ^{4}He core configuration at $\Lambda = 1.97$. For each configuration, the top density corresponds to the ^{3}He crust and the bottom density to the ^{4}He core. The black vertical bars represent a distance of 40 Å. The color bar shows the atom density in units of $Å^{-3}$ and is common to all configurations.

configurations may decay to prolate configurations lying at much lower energy [26].

We have also addressed multiply charged quantum vortices with charge (quantum circulation) $m = 2$–4, and their relative stability with respect to configurations with $n_v = 2$–4 and $m = 1$. In BECs, multiply charged vortices that are stabilized temporarily by the external confining potential have been found [31,32]. In mixed helium droplets, the self-bound thick ^{3}He shell yields a confining potential that plays the same role. In the oblate branch, we have found that, depending on Λ, multiply charged single-vortex configurations with charge m are more stable than arrays of $n_v = m$ singly charged vortices [26], and hence the former cannot decay into the latter as would happen in pure ^{4}He. This is likely due to the presence of ^{3}He in the expanded vortex cores and the ^{3}He crust, which together define a region similar to the rotating annulus used to study quantized superfluid states and vortices in the first experiments on quantized circulation in superfluid ^{4}He [33,34].

Along the prolate branch, we have found metastable configurations with $n_v = 1$–2 where the angular momentum of the ^{4}He core is shared between vortices and capillary waves (see Fig. 3 of [26]). This is similar to what happens in spinning ^{4}He droplets [11,12]. When the ^{4}He core becomes two-lobed, the neck connecting them gets thinner as Λ increases and eventually the most stable configuration is the fissioned one.

Three-lobed configurations were predicted to appear in rotating classical droplets [1]. These configurations are metastable with respect to prolate two-lobed configurations and were not expected to be accessible experimentally. However, three-lobed configurations were obtained [35], stabilized by forcing the droplet into large amplitude periodic oscillations—thus not in gyrostatic equilibrium. Charged ^{4}He drops magnetically levitated have been studied displaying $\ell = 2$–4 oscillation modes induced by a rotating deformation of the droplet [36]. More recently, triangular-shaped magnetically levitated water droplets have been found [37] where the amplitude of the surface oscillation is small and the equilibrium shape could be observed clearly.

In the water droplet experiment, some surfactant was added to water to decrease the surface tension, helping the three-lobed configurations to be formed. In the case of mixed helium droplets, the surface tension of the ^{3}He - ^{4}He interface is already small, hence it is possible to have metastable three-lobed ^{4}He core configurations while the outer surface of the ^{3}He crust is still oblate. Indeed, we have found such configurations in the $1.20 \leqslant \Lambda \leqslant 1.64$ range, one of which is shown in Fig. 4 (see also the central pictogram in Fig. 2). The three-lobed bifurcation sets in at $(\Lambda, \Omega) = (1.20, 0.58)$. We have looked for metastable four-lobed configurations but have not found any, the droplet always decaying into fissioned ^{4}He prolate configurations.

We have thus shown that the presence of a superfluid ^{4}He core inside a normal-fluid ^{3}He nanodroplet produces remarkable changes in its rotational properties. Oblate configurations are affected as the superfluid core cannot participate in the rotation. At variance with rotating pure ^{4}He nanodroplets, oblate vortex-hosting configurations are not the equilibrium ones, as it is energetically more favorable for the droplet to store angular momentum in the deformable ^{3}He crust than in the superfluid ^{4}He core. This happens in the prolate branch as well.

The presence of vortices can be experimentally tested by doping the droplets with heliophilic impurities. These impurities are captured by the droplet and sink into the ^{4}He core [18]. Coherent x-ray scattering would reveal the space distribution of the impurities, which might arrange along the vortex cores if vortex arrays are present [8,12], producing otherwise interference patterns very different from those of vortex-hosting droplets.

Diffractive imaging of fissioned ^{4}He cores should be possible for the $N = 10^8$–10^{11} drops used in ongoing experiments, while it would be challenging for the smaller sizes addressed in this work due to the small contrast between ^{3}He and ^{4}He components. It is less obvious whether metastable three-lobed ^{4}He core configurations may be readily detected; in the case of classical droplets, they were identified 20 years after being predicted. These configurations are highly unstable and can either decay to metastable oblate $n_v = 1$ vortex configurations, or to stable prolate, fissioned core configurations.

We expect that bigger mixed He droplets will accommodate a larger number of vortices in the ^{4}He core. As shown in Refs. [11,12], this will make their rotational behavior closer to that of viscous droplets. The nanoscopic sizes explored in the present work reveal instead many interesting effects of the interplay between the superfluid nature of the ^{4}He core and the ^{3}He coating. Considerable

effort will be needed to reach a range of droplet sizes where both experiments and calculations can be carried out and unveil signatures of quantum effects in their rotation (other than the remarkable presence of vortex arrays) which are not present in viscous drops; in particular, capillary waves.

We are most indebted to Andrey Vilesov for information on his group's ongoing experiments with mixed helium droplets—it has motivated and clarified some aspects of this work. We also thank Sam Butler for useful exchanges. This work has been performed under Grant No. FIS2017-87801-P (AEI/FEDER, UE). J.M.E. acknowledges support from Ministerio de Ciencia e Innovación of Spain through Unidades de Excelencia "María de Maeztu" Grant No. MDM-2017-0767. M.B. thanks the Université Fédérale Toulouse Midi-Pyrénées for financial support through the "Chaires d'Attractivité 2014" Programme IMDYNHE.

[1] R. A. Brown and L. E. Scriven, The shape and stability of rotating liquid drops, Proc. R. Soc. London, Ser. A **371**, 331 (1980).

[2] S. Chandrasekhar, The stability of a rotating liquid drop, Proc. R. Soc. London, Ser. A **286**, 1 (1965).

[3] S. Cohen, R. Plasil, and W. J. Swiatecki, Equilibrium configurations of rotating charged or gravitating liquid masses with surface tension II, Ann. Phys. (NY) **82**, 557 (1974).

[4] K. A. Baldwin, S. L. Butler, and R. J. A. Hill, Artificial tektites: An experimental technique for capturing the shapes of spinning drops, Sci. Rep. **5**, 7660 (2015).

[5] J. P. Toennies and A. F. Vilesov, Superfluid helium droplets: A unique cold nanomatrix for molecules and molecular complexes, Angew. Chem. Phys. **43**, 2622 (2004).

[6] M. Hartmann, R. E. Miller, J. P. Toennies, and A. F. Vilesov, Rotationally Resolved Spectroscopy of SF_6 in Liquid Helium Clusters: A Molecular Probe of Cluster Temperature, Phys. Rev. Lett. **75**, 1566 (1995).

[7] B. G. Sartakov, J. P. Toennies, and A. F. Vilesov, Infrared spectroscopy of carbonyl sulfide inside a pure ^{3}He droplet, J. Chem. Phys. **136**, 134316 (2012).

[8] L. F. Gomez, K. R. Ferguson, J. P. Cryan, C. Bacellar, R. M. P. Tanyag, C. Jones, S. Schorb, D. Anielski, A. Belkacem, C. Bernando *et al.*, Shapes and vorticities of superfluid helium nanodroplets, Science **345**, 906 (2014).

[9] D. Rupp, N. Monserud, B. Langbehn, M. Sauppe, J. Zimmermann, Y. Ovcharenko, T. Möller, F. Frassetto, L. Poletto, A. Trabattoni *et al.*, Coherent diffractive imaging of single helium nanodroplets with a high harmonic generation source, Nat. Commun. **8**, 493 (2017).

[10] B. Langbehn, K. Sander, Y. Ovcharenko, C. Peltz, A. Clark, M. Coreno, R. Cucini, M. Drabbels, P. Finetti, M. Di Fraia *et al.*, Three-Dimensional Shapes of Spinning Helium Nanodroplets, Phys. Rev. Lett. **121**, 255301 (2018).

[11] F. Ancilotto, M. Pi, and M. Barranco, Spinning superfluid ^{4}He nanodroplets, Phys. Rev. B **97**, 184515 (2018).

[12] S. M. O. O'Connell, R. M. P. Tanyag, D. Verma, C. Bernando, W. Pang, C. Bacellar, C. A. Saladrigas, J. Mahl, B. W. Toulson, Y. Kumagai *et al.*, Angular Momentum in Rotating Superfluid Droplets, Phys. Rev. Lett. **124**, 215301 (2020).

[13] F. Ancilotto, M. Pi, and M. Barranco, Vortex arrays in nanoscopic superfluid droplets, Phys. Rev. B **91**, 100503(R) (2015).

[14] D. Verma, S. M. O. O'Connell, A. J. Feinberg, S. Erukala, R. M. Tanyag, C. Bernando, W. Pang, C. A. Saladrigas, B. W. Toulson, M. Borgwardt *et al.*, Shapes of rotating normal fluid ^{3}He versus superfluid ^{4}He droplets in molecular beams, Phys. Rev. B **102**, 014504 (2020).

[15] M. Pi, F. Ancilotto, and M. Barranco, Rotating ^{3}He droplets, J. Chem. Phys. **152**, 184111 (2020).

[16] D. O. Edwards and M. S. Pettersen, Lectures on the properties of liquid and solid ^{3}He - ^{4}He mixtures at low temperatures, J. Low Temp. Phys. **87**, 473 (1992).

[17] S. Grebenev, J. P. Toennies, and A. F. Vilesov, Superfluidity within a small helium-4 cluster: The microscopic Andronikashvili experiment, Science **279**, 2083 (1998).

[18] M. Barranco, R. Guardiola, S. Hernández, R. Mayol, J. Navarro, and M. Pi, Helium nanodroplets: An overview, J. Low Temp. Phys. **142**, 1 (2006).

[19] F. Schreck, L. Khaykovich, K. L. Corwin, G. Ferrari, T. Bourdel, J. Cubizolles, and C. Salomon, Quasipure Bose-Einstein Condensate Immersed in a Fermi Sea, Phys. Rev. Lett. **87**, 080403 (2001).

[20] C. R. Cabrera, L. Tanzi, J. Sanz, B. Naylor, P. Thomas, P. Cheiney, and L. Tarruell, Quantum liquid droplets in a mixture of Bose-Einstein condensates, Science **359**, 301 (2018).

[21] G. Semeghini, G. Ferioli, L. Masi, C. Mazzinghi, L. Wolswijk, F. Minardi, M. Modugno, G. Modugno, M. Inguscio, and M. Fattori, Self-Bound Quantum Droplets of Atomic Mixtures in Free Space, Phys. Rev. Lett. **120**, 235301 (2018).

[22] D. Rakshit, T. Karpiuk, M. Brewczyk, and M. Gajda, Quantum Bose-Fermi droplets, SciPost. Phys. **6**, 079 (2019).

[23] D. S. Petrov, Quantum Mechanical Stabilization of a Collapsing Bose-Bose Mixture, Phys. Rev. Lett. **115**, 155302 (2015).

[24] S. L. Butler, Equilibrium shapes of two-phase rotating fluid drops with surface tension, Phys. Fluids **32**, 012115 (2020).

[25] D. M. Jezek, M. Guilleumas, M. Pi, and M. Barranco, Stability of vortex lines in liquid ^{3}He - ^{4}He mixtures at zero temperature, Phys. Rev. B **55**, 11092 (1997).

[26] See Supplemental Material at http://link.aps.org/supplemental/10.1103/PhysRevB.102.060502 for the energetics and morphologic characteristics of the configurations calculated in this work, the density profile of the vortex-free and vortex-hosting $^4\mathrm{He}_{1500} + {}^3\mathrm{He}_{6000}$ droplet, and several two-dimensional densities of the ^{4}He core displaying the streamlines of the superfluid.

[27] M. Barranco, M. Pi, S. M. Gatica, E. S. Hernández, and J. Navarro, Structure and energetics of mixed ^{4}He - ^{3}He drops, Phys. Rev. B **56**, 8997 (1997).

[28] F. Ancilotto, M. Barranco, F. Coppens, J. Eloranta, N. Halberstadt, A. Hernando, D. Mateo, and M. Pi, Density

functional theory of doped superfluid liquid helium and nanodroplets, Int. Rev. Phys. Chem. **36**, 621 (2017).

[29] M. Pi, F. Ancilotto, F. Coppens, N. Halberstadt, A. Hernando, A. Leal, D. Mateo, R. Mayol, and M. Barranco, 4He-DFT BCN-TLS: A computer package for simulating structural properties and dynamics of doped liquid helium-4 systems, https://github.com/bcntls2016/.

[30] S. L. Butler, M. R. Stauffer, G. Sinha, A. Lilly, and R. J. Spiteri, The shape distribution of splash-form tektites predicted by numerical simulations of rotating fluid drops, J. Fluid Mech. **667**, 358 (2011).

[31] Y. Shin, M. Saba, M. Vengalattore, T. A. Pasquini, C. Sanner, A. E. Leanhardt, M. Prentiss, D. E. Pritchard, and W. Ketterle, Dynamical Instability of a Doubly Quantized Vortex in a Bose-Einstein Condensate, Phys. Rev. Lett. **93**, 160406 (2004).

[32] M. Okano, H. Yasuda, K. Kasa, M. Kumakura, and Y. Takahashi, Splitting of a quadruply quantized vortex in the Rb Bose-Einstein condensate, J. Low Temp. Phys. **148**, 447 (2007).

[33] W. F. Vinen, The detection of a single quantum of circulation in liquid helium II, Proc. R. Soc. Lond. A **260**, 218 (1961).

[34] R. J. Donnelly, *Quantized vortices in Helium II* (Cambridge University Press, Cambridge, UK, 1991).

[35] K. Ohsaka and E. H. Trinh, Three-Lobed Shape Bifurcation of Rotating Liquid Drops, Phys. Rev. Lett. **84**, 1700 (2000).

[36] D. L. Whitaker, M. A. Weilert, C. L. Vicente, H. J. Maris, and G. M. Seidel, Oscillations of charged helium II drops, J. Low Temp. Phys. **110**, 173 (1998).

[37] R. J. A. Hill and L. Eaves, Nonaxisymmetric Shapes of a Magnetically Levitated and Spinning Water Droplet, Phys. Rev. Lett. **101**, 234501 (2008).